Blend Membrane of Regenerated Silk Fibroin, Poly(vinyl alcohol), and Peroxidase and Its Application to a Ferrocene-Mediating Hydrogen Peroxide Sensor

YONGCHENG LIU,[1] JIANGHONG QIAN,[3] HAIYING LIU,[2] XIAOLIN ZHANG,[2] JIAQI DENG,[3] and TONGYIN YU[1,*]

[1]Department of Macromolecular Science, Fudan University, Shanghai 200433, [2]Department of Chemistry and Chemical Engineering, Shanghai University, Shanghai 200072, and [3]Department of Chemistry, Fudan University, Shanghai 200433, People's Republic of China

SYNOPSIS

Before or after the blend membrane of regenerated silk fibroin (RSF), poly(vinyl alcohol) (PVA), and peroxidase is treated with ethanol, RSF, PVA, and peroxidase maintain their own structures. The conformational transition of RSF in the blend membrane is accomplished from the silk I structure to the silk II structure by ethanol treatment, which is used to immobilize peroxidase. A ferrocene-mediating sensor for H_2O_2 is made, which is based on the immobilization of peroxidase in the blend membrane of RSF and PVA. Performance and characteristics of the sensor were evaluated with respect to response time, detection limit, selectivity, and dependencies on temperature and pH as well as on operating and storage stability. © 1996 John Wiley & Sons, Inc.

INTRODUCTION

Interest in the use of polymers as a carrier for immobilizing enzymes has existed for a long time. The immobilized enzymes have been applied to bioprocessing,[1,2] analytic systems,[3] etc. According to different usages, the polymers for immobilizing enzymes are available in many different physical forms, such as fiber,[4,5] microspheres,[6-10] gels,[11-13] and membranes.[14-18] In the use of biosensors, enzymes are generally immobilized onto the polymer membranes. In recent years, many methods have been developed to immobilize enzymes onto the electrode surface as onto amperometric sensors. They include physical adsorption, chemical bending (crosslinking), electrostatic attraction (ion exchange), and entrapment. The polymers as an immobilization matrix of enzymes include artificial and natural polymers, such as poly(acryl amide), poly (methyl methacrylate), poly(styrene sodium sulfonate), chitosan, K-carrageenan, chitin, collagen, gelatin, poly(acrylamide-*co*-Na acrylate), and polypyrrole. Recently, we successfully immobilized glucose oxidase[19] and peroxidase[20] by using regenerated silk fibroin (RSF) as an immobilization matrix. As a biomaterial, RSF has many advantages over other natural and synthetic materials, such as its biological compatibility and stability to most solvents. As an enzyme immobilization matrix, its major merit is that it entraps enzymes without using the usual crosslinking chemicals. The process is accomplished by physical, chemical, or mechanical treatment. Immobilization of enzymes is based on its conformational transition from a water-soluble silk I structure to a water-insoluble silk II structure. However, it becomes brittle in organic solvents or in a dried state for a long time. To improve its mechanical property, we prepared a blend of RSF and poly(vinyl alcohol) (PVA). The blend maintains the excellent property of RSF and possesses better mechanical properties. Moreover, it has been used to immobilize glucose oxidase.[21] In this article, we explored the feasibility that the blend of RSF and PVA is used to immobilized peroxidase, investigated the structure of the blend membrane

* To whom correspondence should be addressed.

Journal of Applied Polymer Science, Vol. 61, 641-647 (1996)
 CCC 0021-8995/96/040641-07

of RSF, PVA, and peroxidase, and examined the parameters of the hydrogen peroxide sensor based on ferrocene's mediating electron transfer between immobilized peroxidase and a glassy carbon electrode.

EXPERIMENTAL

Materials

Peroxidase from horseradish (POD) (EC 1.11.1.7, type VI) and ferrocene were obtained from Sigma. A solution of the Eastman-AQ-55D polymer (28% dispersion) was obtained from Eastman Kodak Co. Hydrogen peroxide (30% w/v solution) and PVA was purchased from Shanghai Chemical Reagent Co. The concentration of these diluted peroxide solutions prepared from this material was determined by titration with cerium(IV) to a ferroin endpoint.[22] Regenerated fibroin solution was prepared according to the literature.[19] All other chemicals were of analytical grade. All the solutions were prepared with deionized water. Membranes were cast by using the RSF solution or the mixed solution of the given weight of the silk fibroin, PVA, and peroxidase on glass plates at room temperature in air.

Fabrication of Eastman-AQ-Ferrocene-modified Electrode

The glassy carbon electrodes were polished with 0.3, 0.1, and 0.05 μm Al_2O_3, rinsed thoroughly in deionized water between each polishing step, sonicated in 1 : 1 nitric acid, acetone, and doubly distilled water consecutively, and dried in air before use. Eastman-AQ-ferrocene was coated onto the electrode by pipetting 8 μL of diluted Eastman-AQ (1 : 25 (v/v Eastman-AQ : acetone) polymer solution containing 0.06*M* ferrocene onto the electrode surface and letting it dry in air.

Construction of Hydrogen Peroxide Sensor

Twenty milligrams peroxidase was completely dissolved in a 0.6 mL blend solution of RSF and PVA. Aliquots (30 μL) of the mixture were spread onto the Eastman-AQ-ferrocene modified electrode and allowed to dry in ambient conditions for 20 h and then 2 μL of a 2% Eastman-55D ethanol-diluted solution was pipetted onto the surface of the sensor, letting it dry. The sensor was kept dry in air at 4°C in a refrigerator between the measurements.

Pretreatment of Hydrogen Peroxide Sensor

After fabrication of the sensor and prior to experiments, the sensor response was stabilized by scanning between +0.5 and −0.2 V (vs. SCE) in phosphate buffer (pH 6.0) over a 10 min period. During this process, ferrocene (Fc) was oxidized to Fc^+ and incorporated into Eastman-AQ polymer by ion exchange. The electrochemical reaction of ferrocene in the Eastman-AQ film can be described as follows:

$$Fc + SO_3/Na^+ \rightarrow SO_3/Fc^+ + Na^+ + e.$$

Measurements

IR spectra of the dried membranes were recorded by the transmission method on a MAGNA-IR 550 (Nicolet) spectrometer at room temperature. All experiments were performed with a three-electrode system comprising a hydrogen peroxide sensor as a working electrode, a saturated calomel reference electrode (SCE), and a platinum wire auxiliary electrode. The electrodes were connected to an FDH 3204 and FDH 3206 cyclic voltammetry apparatus (Scientific Equipment Co. of Fudan University, China) and the signal was recorded on a type 3086 $x - y$ recorder (Tokyo, Japan) for cyclic voltammetric and amperometric measurements, separately. All experiments were carried out in a thermostatted stirred electrochemical cell containing 5 mL of 0.1*M* phosphate buffer (pH 7.0) at 25.0 ± 0.5°C. In the constant potential experiments, aliquots of the hydrogen peroxide stock solution were successively injected into the cell while the current was monitored after a constant residual current had been established. A calibration curve was obtained by applying a standard addition method, with measurements at 95% of the steady-state current.

DISCUSSION AND RESULTS

Structure of Samples

Figure 1 shows the IR spectra of the membranes before ethanol treatment. The blend membrane of RSF, PVA, and peroxidase displays the absorption bands at 1654 cm^{-1} (amide I), 1540 cm^{-1} (amide II), and 1237 cm^{-1} (amide III) [shown in Fig. 1(D)], which is assigned to the silk I structure of RSF since the absorption bands of the pure RSF membrane are 1653 cm^{-1} (amide I), 1543 cm^{-1} (amide II), and 1243 cm^{-1} (amide III) [shown in Fig. 1(A)], which is characteristic of the silk I structure. The absorp-

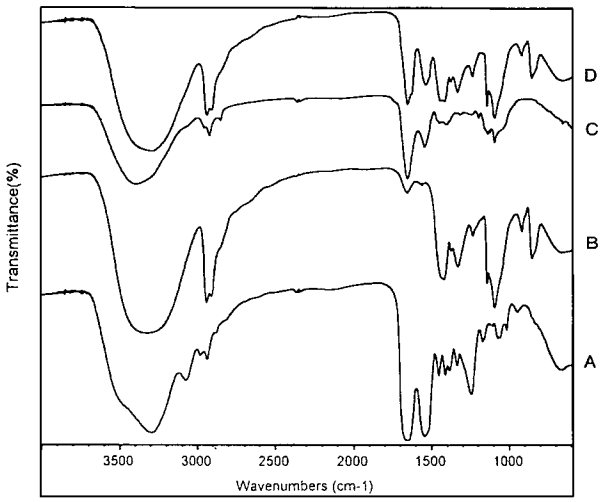

Figure 1 IR spectra of the samples before ethanol treatment: (A) RSF; (B) PVA; (C) POD; (D) RSF : PVA : POD = 4 : 20 : 3.

tion bands at 1443 and 1334 cm^{-1} in the blend membrane [shown in Fig. 1(D)] are attributed to the O — H bending absorption bands of PVA since pure PVA displays the absorption bands at 1446 and 1332 cm^{-1} (O — H bending) [shown in Fig. 1(B)]. The absorption bands at 1143 and 1094 cm^{-1} [shown in Fig. 1(D)] are attributed to the C — O stretching absorption bands of PVA since pure PVA illustrates the absorption bands at 1142 and 1093 cm^{-1} (C — O stretching) [shown in Fig. 1(B)]. The absorption bands of peroxidase at 1655 and 1544 cm^{-1} [shown in Fig. 1(C)] are overlapped by the ones of RSF in the blend membrane. These facts indicate that the RSF, PVA, and peroxidase, respectively, maintain their own structures in the blend membrane before ethanol treatment.

Figure 2 shows IR spectra of the membranes after ethanol treatment. The blend membrane of RSF, PVA, and peroxidase displays the absorption bands at 1626 cm^{-1} (amide I), 1527 cm^{-1} (amide II), and 1235 cm^{-1} (amide III) [shown in Fig. 2(D)], which is attributable to the silk II structure of RSF because the characteristic absorption bands of the silk II structure of pure RSF are 1627 cm^{-1} (amide I), 1531 cm^{-1} (amide II), and 1236 cm^{-1} (amide III) [shown in Fig. 2(A)]. The absorption bands at 1444 and 1333 cm^{-1} in the blend membrane [shown in Fig. 2(D)] are assigned to the O — H bending absorption bands of PVA because pure PVA displays the absorption bands at 1448 and 1334 cm^{-1} (O — H bending) [shown in Fig. 2(B)]. The absorption bands at 1142 and 1093 cm^{-1} are attributed to the C — O stretching absorption bands of PVA because pure PVA illustrates the absorption bands at 1144 and 1093 cm^{-1} (C — O stretching) [shown in Fig. 2(B)]. These facts show that the RSF, PVA, and peroxidase in the blend membrane still maintain their own structures, respectively, in spite of ethanol treatment.

Electrochemical Characterization of Hydrogen Peroxide Sensor

Figure 3 gives cyclic voltammograms of the H_2O_2 sensor at various scan rates in 0.1*M* phosphate buffer (pH 7.0). Without H_2O_2 in solution, the enzyme contributes no response and only the ferrocene-generated voltammograms comply with a reversible electron redox agent (ΔE_p = 60 mV [25°C]; $ip/v^{1/2}$ constant). The blend membrane of regenerated silk, PVA, and peroxide does not affect the electrochemical behavior of ferrocene since the mediator couple remains reversible in the presence of the enzyme film.

Bioelectrocatalytic Reduction of Hydrogen Peroxide at Sensor

There is no electrocatalytic reduction current at the Eastman-AQ-ferrocene-modified electrode upon addition of H_2O_2 to the phosphate buffer. Figure 4 shows characteristic cyclic voltammetric results for the H_2O_2 sensor. In the absence of H_2O_2, only a typical oxidation and reduction peak for ferrocene at the electrode in solution is observed [Fig. 4(a)]. Adding H_2O_2 to the cell brings about an enhanced reduction peak current for ferrocene. Comparison

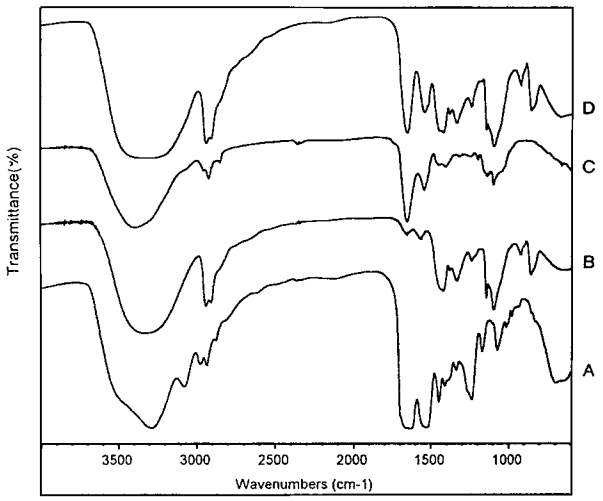

Figure 2 IR spectra of the samples after ethanol treatment: (A) RSF; (B) PVA; (C) POD; (D) RSF : PVA : POD = 4 : 20 : 3.

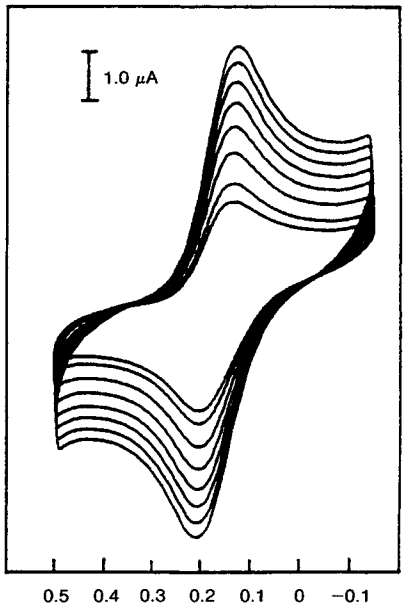

Figure 3 Cyclic voltammograms of the sensor for hydrogen peroxide at various scan rates of 15, 25, 45, 65, 85, 105, 125, 145, and 165 mV/s (from inner curve to outer one) in 0.1*M* phosphate buffer.

of the voltammograms in the absence and presence of H_2O_2 demonstrates that ferrocene can enhance electron communication between immobilized peroxidase and a glassy carbon electrode.

Peroxidase from horseradish is a glycoprotein with a molecular weight of approximately 44,000 (Ref. 23) containing ferroprotoporphyrin IX as the strongly bound cofactor. Horseradish peroxidase (HRP) is known to catalyze the reduction of hydrogen peroxide and certain organic peroxides. In a single two-electron process, the native form of HRP is oxidized by hydrogen peroxide to form water and an oxidized form of HRP:

$$\text{HRP} + \text{H}_2\text{O}_2 \rightarrow \text{compound I} + \text{H}_2\text{O}$$

The reduction of compound I to HRP can be achieved through two successive one-electron steps[24,25] by employing an electron transfer mediator or by direct electron transfer from the electrode to the heme site of the HPR in intimate contact with the conducting surface in the absence of a mediator:

$$\text{compound I} + \text{Med}_{\text{red}}\ (\text{or } e^-) \rightarrow \text{compound II} + \text{Med}_{\text{ox}}$$

$$\text{compound II} + \text{Med}_{\text{red}}\ (\text{or } e^-) \rightarrow \text{HRP} + \text{Med}_{\text{ox}}$$

The oxidized mediator can be reoxidized and recycled at the electrode, resulting in a reduction current:

$$\text{Med}_{\text{ox}} + 2e \rightarrow \text{Med}_{\text{red}}$$

Moreover, employing a mediator in a biosensor can significantly improve the sensitivity of the biosensor toward hydrogen peroxide.

Steady-state Amperometric Response of the Sensor to H_2O_2

The steady-state response of the sensor to H_2O_2 is measured at an applied potential 0 V (vs. SCE) (Fig. 5). The curve (current vs. time) clearly illustrates the quick response and high sensitivity of the sensor to H_2O_2. The sensor reaches steady-state current

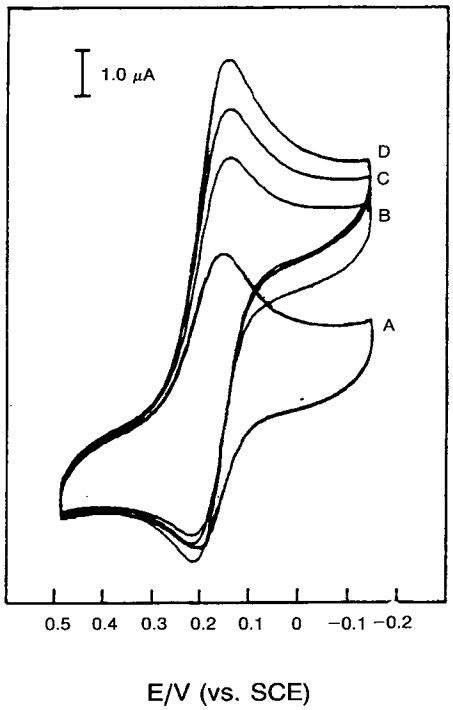

Figure 4 Cyclic voltammograms of the H_2O_2 sensor at a scan rate of 65 mV/s in 0.1*M* phosphate buffer (pH 7.0) (a) without H_2O_2 and with H_2O_2 concentration of (b) 0.05, (c) 0.075, and (d) 0.1 m*M* H_2O_2.

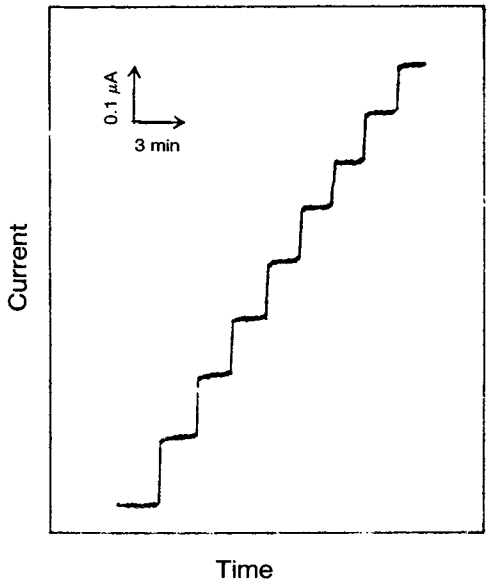

Figure 5 Dynamic response of the H_2O_2 sensor to successive addition of H_2O_2 in 50 μM steps in solution at the applied potential of 0.0 V.

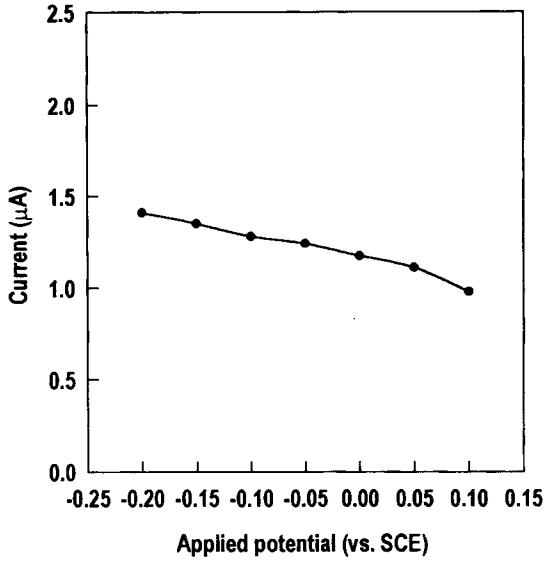

Figure 7 Effect of applied potential on the response of the sensor to H_2O_2; the experiment was carried out in 0.1M phosphate buffer containing 0.5 mM H_2O_2.

responses within 50 s after adding the stock H_2O_2 solution. The fast response of the sensor to H_2O_2 results from the enhanced hydrophilicity of the blend membrane of RSF and PVA, which reduces the mass-transfer resistance to the substrate and reaction product. Figure 6 displays the plot of current response as a function of H_2O_2 concentration.

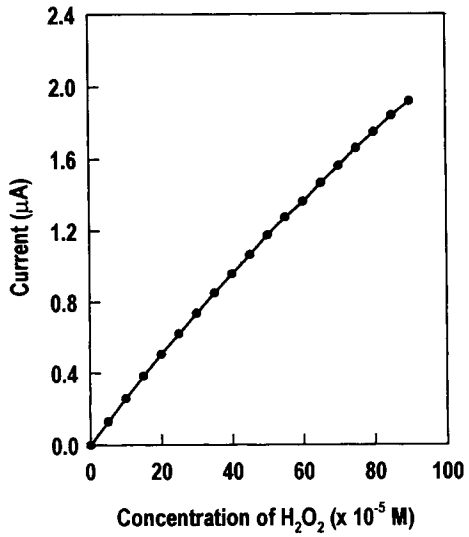

Figure 6 Calibration plot for the H_2O_2 sensor.

The sensor has a detection limit of 0.1 μM at a signal-to-noise ratio of 3.

Figure 7 shows the effect of the applied potential on the sensor response to 0.5 mM H_2O_2. The current response of the sensor increases on stepping the applied potential from 0.1 to −0.2 V (vs. SCE). The increased sensitivity with a decreasing applied potential can be ascribed to the increased driving force for the fast reduction of compounds I and II of HRP. At an applied potential of 0.3 V, the reduction current keeps increasing even without hydrogen peroxide, which is attributed to the fact that the dissolved oxygen in the buffer starts to be reduced at the potential. The working potential is fixed at 0.0 V for all other experiments, where electroactive species such as ascorbic acid and uric acid are neither oxidized nor reduced at the electrode.

Dependence of the Sensor on pH and Temperature

The effect of pH on the sensor is shown in Figure 8, displaying an optimum pH between 6.0 and 6.5, which indicates that the pH profile is controlled by the enzymatic activity. The influence of temperature on the sensor was investigated between 15 and 60°C. The experiment shows that the current response of the sensor increases with temperature, reaching a maximum value at about

50°C. Further increasing temperature results in a decrease in response current because of the partial denaturation of the enzyme.

Stability of the Sensor

The storage stability of the sensor stored at 4°C was studied by checking periodically its relative activity (Fig. 9). The activity is maintained 96.5% for 1 month and 90.5% for 2 months storage. The operational stability was examined by recording over 25 successive assays of 0.5 and 0.3 m*M* H_2O_2; the relative standard deviations are 2.8 and 3.3%, respectively.

CONCLUSION

The blend of RSF and PVA was successfully used to immobilize peroxidase. In the blend membrane of RSF, PVA, and peroxidase, each maintains their own intrinsic properties. We developed a reliable, low-cost, highly sensitive sensor for H_2O_2 by employing ferrocene as an electron shuttle between immobilized peroxidase in the blend membrane and a glassy carbon electrode. While the method is demonstrated in connection with peroxidase, it could be extended to other enzymes or to other bioactive materials.

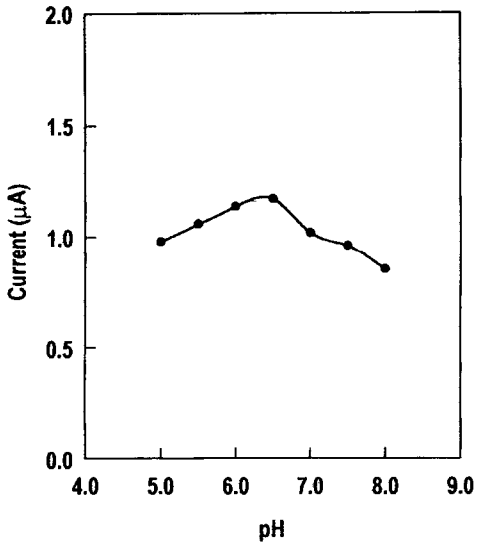

Figure 8 Effect of pH on H_2O_2 sensor; the experiment was conducted in 0.1*M* phosphate buffer containing 0.5 m*M* H_2O_2.

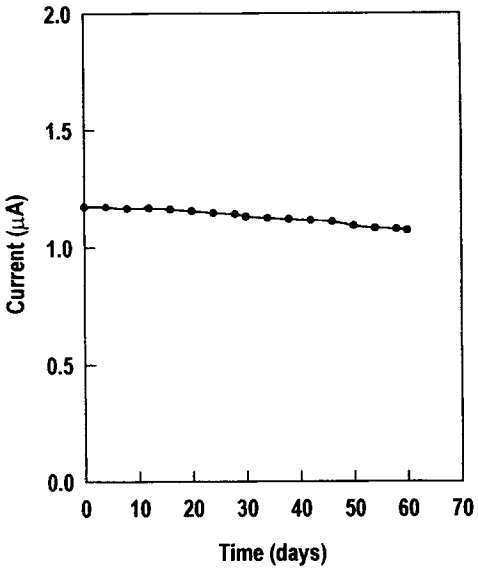

Figure 9 Stability of the H_2O_2 sensor under dry storage at 4°C.

This work was supported by the Key Basic Topics of China, the National Science Foundation of China, and the Electroanalytical Chemistry Open Laboratory of the Changchun Institute of Applied Chemistry, and the Chinese Academy of Science.

REFERENCES

1. P. Linko and Y. Y. Linko, *Crit. Rev. Biotechnol.*, **1**, 289 (1984).
2. I. Chibata, T. Tosa, and T. Sato, in *Biotechnology, Enzyme Technology,* J. F. Kennedy, Ed., VCH Vertagsgesellschaft, Weinheim, 1987, Vol. 7a, p. 653.
3. I. Karube, in *Biotechnology, Enzyme Technology,* J. F. Kennedy, Ed., VCH Verlagsgesellschaft, Weinheim, 1987, Vol. 7a, p. 685.
4. D. Dinelli, W. Marconi, and F. Morisi, in *Methods in Enzymology: Immobilized Enzymes,* K. Mosbach, Ed., Academic Press, New York, 1976, Vol. 44, p. 227.
5. E. Drioli, NATO ASI Ser., Ser. C (*Synth. Memb. Sci., Eng. Appl.*), 667 (1986).
6. A. Bahadur, P. Bahadur, and G. Riess, *Makromol. Chem.*, **186,** 1387 (1985).
7. T. Hayashi and Y. Ikada, *J. Appl. Polym. Sci.*, **42,** 85 (1991).
8. T. Hayashi, C. Hirayama, and M. Iwamatsu, *J. Appl. Polym. Sci.*, **44,** 143 (1992).
9. T. Hayashi, *Makromol. Chem., Macromol. Symp.*, **70–71,** 137 (1993).
10. K. Ampon, *J. Chem. Technol. Biotechnol.*, **55,** 185 (1992).

11. L. Tarhan, H. Arif, and U. Slan, *J. Fac. Sci., Ege Univ., Ser. A,* **14,** 11 (1991).
12. R. F. Boyer and J. S. McArthur, *Biotechnol. Ed.,* **2,** 17 (1991).
13. F. Liu and R. Zhao, *Biotechnol. Appl. Biochem.,* **18,** 57 (1993).
14. S. K. Dalvie and R. E. Battus, *Biotechnol. Bioeng.,* **40,** 1173 (1992).
15. P. N. Bartlett and J. M. Cooper, *J. Electroanal. Chem.,* **362,** 1 (1993).
16. W. Schuhmann, *Bioelectroanal. Symp.,* **2,** 113 (1992).
17. J. Wang, Q. Chen, and C. L. Reuschler, *Anal. Chem.,* **66,** 1988 (1994).
18. A. Ohki, K. Naka, O. Ito, and S. Maeda, *Chem. Lett.,* **6,** 1065 (1994).
19. T. Yu, H. Liu, J. Deng, and Y. Liu, *J. Appl. Polym. Sci.,* to appear.
20. Y. Liu, H. Liu, J. Qian, J. Deng, and T. Yu, *Electrochim. Acta,* to appear.
21. H. Liu, J. Qian, Y. Liu, T. Yu, and J. Deng, *Bioelectrochem. Bioener.,* to appear.
22. E. C. Hurdis and H. Romeyn, Jr., *Anal. Chem.,* **26,** 320 (1954).
23. K. J. Welinder, *Eur. J. Biochem.,* **96,** 483 (1979).
24. H. Yamada and I. Yamazaki, *Arch. Biochem. Biophys.,* **165,** 728 (1974).
25. A. C. Maehly, *Methods Enzymol.,* **2,** 801 (1955).

Received August 28, 1995
Accepted December 19, 1995